REFOLDING OF THIN-SKINNED THRUST SHEETS BY ACTIVE BASEMENT-INVOLVED THRUST FAULTS IN THE EASTERN PRECORDILLERA OF WESTERN ARGENTINA

Andrew MEIGS[1], William C KRUGH[2], Celia SCHIFFMAN[1], Jaume VERGÉS[3] and Victor A. RAMOS[4]

[1] Department of Geosciences, Oregon State University, Corvallis, OR, 97331, U.S.A.
[2] Earth Science, Institute of Geology, ETH Zentrum, Sonneggstrasse 5, CH-8092 Zurich, Switzerland.
[3] Institute of Earth Sciences "Jaume Almera", CSIC, Lluís Solé i Sabarís s/n, 08028 Barcelona, Spain.
[4] Laboratorio de Tectónica Andina, Departamento de Ciencias Geológicas, Universidad de Buenos Aires, 1428 Buenos Aires, Argentina

ABSTRACT

Devastating earthquakes like the 1944 San Juan earthquake reflect active deformation in western Argentina. Although the earthquake caused considerable damage to San Juan, the source of the earthquake remains uncertain. Potential source faults occur in the thin-skinned fold-and-thrust belt Precordillera province and in the thick-skinned Sierras Pampeanas province, to the west and east, respectively of Sierra de Villicum, a thrust sheet in the eastern Precordillera northwest of San Juan. Sierra de Villicum is a west-vergent thrust sheet bound on the northwest by the Villicum thrust, which juxtaposes a southeast dipping panel of Cambro-Ordovician and Neogene strata in the hanging wall with Neogene red beds in the footwall. A series of Late Pleistocene fluvial terraces developed across the Villicum thrust show no evidence of active fold or fault deformation. Terraces are deformed by active folds and faults in the middle of the southeastern flank of the Sierra de Villicum thrust sheet. A southeast-facing, southwest-plunging monocline characterizes the Neogene red beds in the region of active folding. Co- and post-seismic surface rupture along roughly 6 km of the La Laja fault in 1944 occurred in the limb of the monocline. Evidence that surface deformation in the 1944 earthquake was dominated by folding includes terrace´s fold geometry, which is consistent with kink-band models for fold growth, and bedding-fault relationships that indicate that the La Laja fault is a flexural slip fault. A blind basement reverse fault model for the earthquake source and for active deformation reconciles the zone of terrace deformation, coseismic surface rupture on the La Laja fault, refolding of the Villicum thrust sheet, a basement arch between the Precordillera and eastern Precordillera, and microseismicity that extends northwestward from a depth of ~5 km beneath Sierra de Villicum to ~35 km depth. Maximum horizontal shortening rate is estimated to be ~3.0 mmyr^{-1} from the terrace fold model and correlation of the terraces with dated terraces located to the southwest of the study area. Basement rocks beneath Cerro Salinas, another eastern Precordillera thrust sheet to the southwest, are also characterized by an east-facing monoclinal geometry, which suggests that blind thrust faulting on east-vergent basement faults represents a significant, underappreciated seismic hazard in western Argentina.

Keywords: *Neotectonics, San Juan, La Laja, Villicum, flexural slip fault, 1944 earthquake.*

RESUMEN: *Replegamiento de láminas de corrimiento epidérmicas mediante fallas inversas de basamento activas en la Precordillera Oriental del oeste de Argentina.*

La deformación activa en el oeste de Argentina está reflejada por terremotos devastadores como el sismo de San Juan en 1944. Aunque el terremoto causó un daño considerable a San Juan, la fuente del terremoto permanecía incierta. Fuentes potenciales de falla ocurren en las fajas plegadas y corridas adyacentes, la epidérmica de la Precordillera o la faja de basamento de Sierras Pampeanas, al oeste y este respectivamente de la sierra de Villicum, una lámina de corrimiento de la Precordillera Oriental, ubicada al noroeste de la provincia de San Juan. La sierra de Villicum es una lámina de corrimiento limitada al oeste por el corrimiento de Villicum, que yustapone un panel de estratos cambro-ordovícicos y neógenos de la pared colgante, con estratos rojos neógenos en la pared yaciente. Una serie de terrazas fluviales desarrolladas a través del corrimiento de Villicum no tienen evidencia activa de plegamiento o falla. Las terrazas están deformadas por fallas y pliegues activos en el medio del flanco sudeste de la lámina de corrimiento de la sierra de Villicum. La región de replegamiento activo está caracterizada por un monoclinal buzante al sudoeste de estratos neógenos que inclinan al sudeste. Rupturas superficiales cosísmicas y postsísmicas de la falla de La Laja ocurrieron en 1944 a lo largo de aproximadamente 6 km en el limbo del monoclinal. La evidencia de deformación superficial en el terremoto de 1944 estuvo dominada por plegamiento, incluido el de terrazas con geometría de pliegues, las que son consistentes con modelos de kink-bands para pliegues de crecimiento y con relaciones de fallas de estratificación que indican que la falla de La Laja es una falla por flexo deslizamiento. Un modelo de falla inversa ciega en el basamento para la fuente del terremoto y para la deformación activa, reconcilia la deformación en la zona de terrazas, la ruptura superficial cosísmica en la falla de La Laja, el repliegue de la lámina de corrimiento de Villicum, el arqueamiento del basamento entre la Precordillera y la Precordillera Oriental y la sismicidad que se extiende en profundidad hacia el noroeste desde ~5 km a unos ~35 km por debajo de la sierra de Villicum. La tasa de acortamiento horizontal máximo es estimada en unos ~3,0 mm por año a partir del modelo de plegamiento de terraza y su correlación con las terrazas datadas ubicadas al sudoeste del área estudiada. Rocas de basamento por debajo del cerro Salinas, una lámina de corrimiento de las Sierras Pampeanas ubicada al sudoeste de la región estudiada, también está caracterizada por una geometría monoclinal inclinada al este, que sugiere que fallas inversas ciegas en fallas de basamento con vergencia oriental representan un riesgo sísmico significativo, pero subvalorado en el oeste de Argentina.

Palabras clave: *Neotectónica, San Juan, La Laja, Villicum, falla flexo-deslizante, terremoto de 1944.*

0004-4822/02 $00.00 + $00.50

INTRODUCTION

On January 15th, 1944 San Juan, Argentina experienced a devastating Ms 7.4 earthquake. Whereas the precise location, depth, and focal mechanism of the earthquake are poorly known, post-earthquake field surveys revealed surface deformation on the eastern flank of Sierra de Villicum. (Bastías *et al.* 1985, Groeber 1944, Harrington 1944, Paredes and Uliarte 1988). Harrington (1944) documented 30 cm of vertical coseismic and 30 cm of postseismic displacement along ~6km of the La Laja fault. Sierra de Villicum is the hanging wall of one of a series of thrust sheets comprising the eastern Precordillera structural province, which sits between the thin-skinned Precordillera fold-and-thrust belt on the west and the thick-skinned Sierras Pampeanas structural province on the east (González Bonorino 1950) (Fig. 1). Three faults have been suggested as the seismogenic source of the earthquake. Surface rupture on the La Laja fault identifies it as a candidate structure (Alvarado and Beck 2006, Bastias *et al.* 1985, Perucca and Paredes 2000, 2002). A second potential candidate is the southeast-dipping thrust, the Villicum thrust, which bounds the northwestern flank of Sierra de Villicum (Siame *et al.* 2002), which juxtaposes Cambrian carbonates with Neogene red beds (Ragona *et al.* 1995). Microseismicity beneath the range suggests that a third possibility is a basement fault zone that strikes northeast, dips northwest, and extends from 5 to 35 km depth (Smalley *et al.* 1993). Thus, alternative models for the source of the 1944 event include surface rupturing thin-skinned faults (La Laja or the Villicum fault) or a blind thick-skinned thrust.

In this paper, we merge new field mapping of fluvial terraces and bedrock structure, structural models of fold growth, and published seismicity in a new model for the crustal structure of the transition between the thin-skinned fold-and-thrust belt and the thick-skinned thrust province in the foothills between the Andes and the Sierras Pampeanas in western Argentina. Field relationships indicate that the fault system along the northwestern range front of Sierra de Villicum does not cut a suite of fluvial terraces; equivalent terraces, however, are deformed by an east-facing monocline and surficial thrust faults on the southeast flank of the range. Within this region of active folding and faulting, flexural slip faulting characterizes some of the active faults, including the La Laja fault, which indicates these are secondary faults related to folding. When this observation is combined with field data indicating the southeastern flank of Sierra de Villicum defines a broad, southeast-facing anticlinorium, these data support the inference that the seismogenic source of the 1944 event occurred on a blind, northwest-dipping thrust in the basement. Moreover, comparison with other active structures along strike suggests that active deformation in the basement refolds earlier emplaced thin-skinned thrust sheets. If correct, this interpretation has local implications for the tectonic development of the eastern Precordillera structural

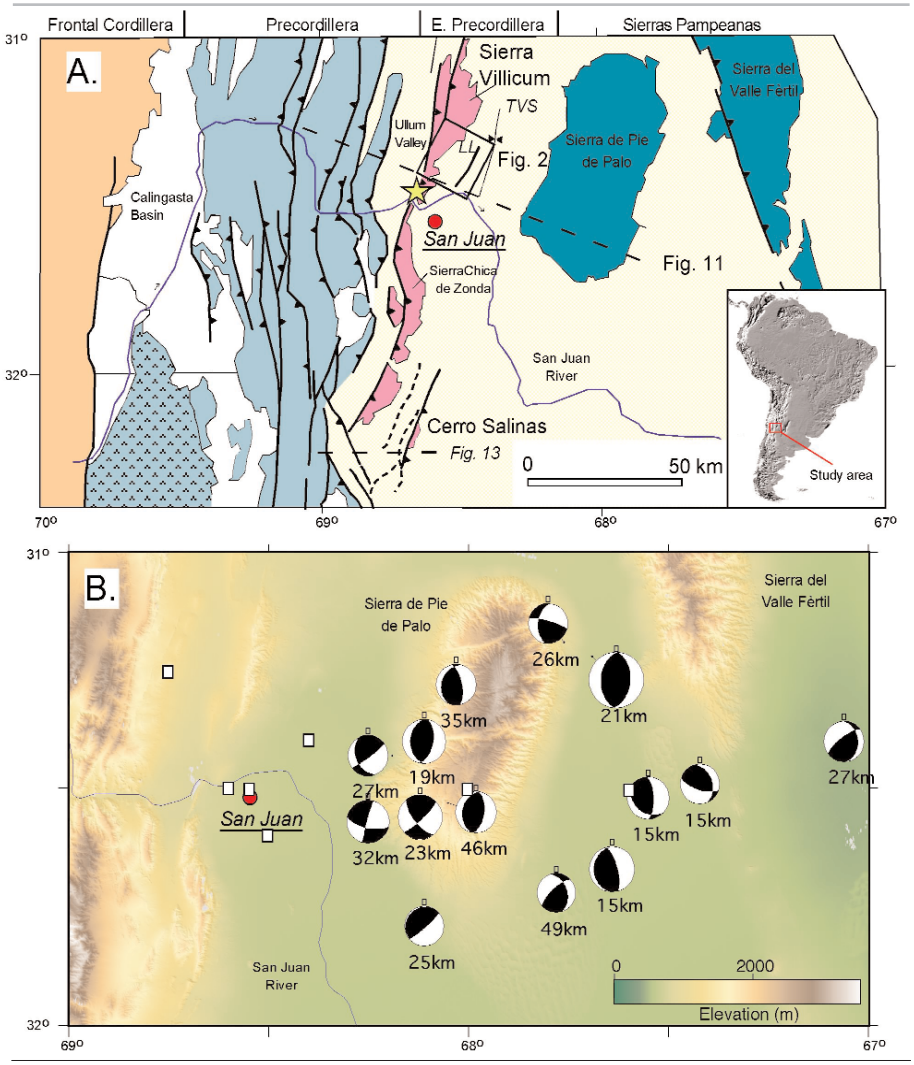

Figure 1: a) Regional tectonic map of Argentine Andes between 31° and 32° south. Four structural provinces comprise the crustal structural at this latitude, including the Frontal Cordillera (beige), the Precordillera (pale green), an east vergent thin-skinned fold-and-thrust belt, the eastern Precordillera (pink), a zone of west vergent thrust sheets, and the thick-skinned Sierras Pampeanas (turquoise) structural provinces in the vicinity of San Juan, Argentina (modified from Ragona *et al.* 1995). LL marks the La Laja fault and TVS indicates the Tulum Valley Syncline. A box marks the location of the map in figure 2. Yellow star marks the location of terraces dated by Siame *et al.* (2002). Cross-section location in figures 11 and 13 are indicated. b) Shaded relief map of the San Juan region showing focal mechanisms of historical seismicity (1977 to the present) for shallow crustal events (<50km) from the Harvard Centroid Moment Tensor Catalog. Depth is given below beach balls. White boxes are 1944 earthquake epicentral locations summarized in Alvarado and Beck (2006).

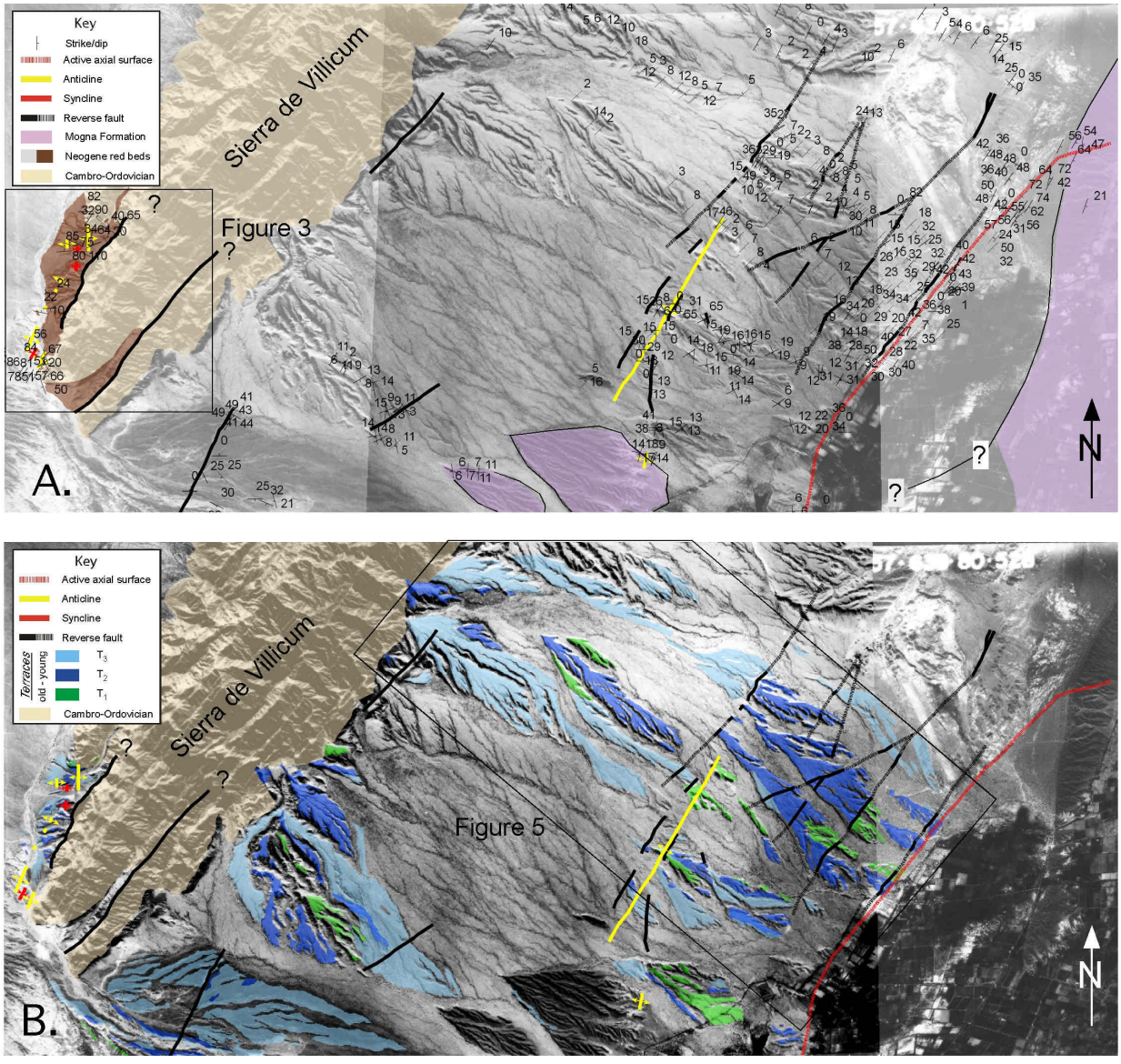

Figure 2: a) Bedrock geologic map of the southwestern end of Sierra de Villicum. Brown shading of Neogene redbeds highlights repetition of Cambro-Ordovician-Neogene red bed thrust imbricates. Grey color used to show Neogene red bed distribution on southeast flank. b)Terrace map. The locations of figures 3 and 5 are shown. Structural data are omitted from (b) to highlight distribution of terraces. Note that thrust faults at southwestern end of Sierra de Villicum do not extend southwestward into Neogene red beds.

transition region, seismic hazard for large cities along the eastern foothills of the Andes in Argentina, and global implications for understanding the development of thick-skin thrust structural provinces and for recognition of blind thrust fault seismic hazards.

THRUST ARCHITECTURE BETWEEN THE PRECORDILLERA AND SIERRAS PAMPEANAS

Outcrops in the Precordillera, eastern Precordillera, and Sierras Pampeanas constrain the stratigraphic location and depth of the principal thrust systems. Ordovician and younger rocks are exposed in the Precordillera (Ragona *et al.* 1995, von Gosen 1992) (Fig. 1), which forms the basis for the interpretation that the Precordillera is an east-vergent thin-skinned thrust belt with a basal décollement in Orodovician-Lower Devonian sediments (Cristallini and Ramos 2000, von Gosen 1992). Precambrian and early Paleozoic basement rocks are exposed in Pie de Palo and other ranges in the Sierras Pampeanas province farther east (González Bonorino 1950). Historic earthquakes, structural geometry, and active faults indicate that east-dipping, west-vergent basement-involved faults are the dominant structure of the Sierras Pampeanas province (Costa *et al.* 1999, Costa and Vita-Finzi 1996, Jordan and Allmendinger 1986, Jordan *et al.* 1983a, b, Kadinsky-Cade *et al.* 1985, Ramos *et al.* 2002, Zapata and Allmendinger 1996b). Bedrock geology indicates that many of the basement faults bounding the Sierras Pampeanas ranges are reactivated Paleozoic and

older sutures and terrane boundaries (Ramos *et al.* 2002). Eastern Precordillera thrust sheets define a narrow belt between east-directed thrust sheets of the Precordillera and west-directed basement reverse faults of the Sierras Pampeanas (Fig. 1). Strata exposed at the base of east-dipping thrust sheets are restricted to Cambro-Ordovician carbonates (Fig. 2). Thus, the eastern Precordillera has characteristics in common with the Precordillera, in that cover sedimentary rocks are exposed in thrust sheets at the surface and characteristics in common with Pampean range thrusts, in that faults dip east. Whether the eastern Precordillera has a thin-skinned structural style, in which upper plate faults root to a décollement at the base of Cambrian strata or into the basement is unresolved (Alvarado and Beck 2006, Ramos *et al.* 2002, Siame *et al.* 2002, von Gosen 1992).

Sierra de Villicum is a N-S trending range located in the eastern Precordillera (Fig. 1). Bedrock structure exposed in the core of the range reveals a series of west-vergent imbricate thrust sheets involving an Upper Cambrian through Middle Miocene stratigraphic sequence (Fielding and Jordan 1988, von Gosen 1992). An angular unconformity marks the contact between steeply-tilted Cambro-Ordovician rocks and overlying moderately-tilted Neogene red beds (Figs. 2a and 3) (von Gosen 1992). A range front fault system, the Villicum thrust fault (Siame *et al.* 2002, von Gosen 1992), marks the contact between folded Neogene red beds in the footwall and the Cambro-Ordovician sequence in the hanging wall along the northwestern flank of the range (Figs 2a and 3). On the southeastern flank of Sierra de Villicum, an angular unconformity separates the Cambro-Ordovician rocks from shallowly dipping Neogene conglomerates, sandstones, and siltstones (Krugh 2003). A second unconformity marks the contact between the Neogene red beds and the overlying Mogna Formation, a conglomerate characterized by abundant volcanic and plutonic clasts (Fig. 2a).

Five terraces were identified around the periphery of Sierra de Villicum (Fig. 2b). An individual terrace comprises an erosional surface on bedrock, a strath, and an overlying capping gravel, typically 1-3 meters thick (Krugh 2003). Clast composition of the capping gravels is dominated by limestone, dolostone, and chert. Gravel in terraces on the southwest end of Sierra de Villicum includes volcanic and plutonic clasts as well. The relative ages of the terraces were determined by their distribution, strath elevation above modern channels, and differences in surface morphology and composition. Sequentially younger terraces are inset into older terraces and occupy lower elevations with respect to modern channels. Older terraces are more dissected, have lower surface relief, and have a higher concentration of varnished chert clasts. Based on these observations, the terraces were classified T1 = oldest to T5 = youngest. Four of the terraces (T1-4) are regionally extensive, well preserved around the periphery of Sierra de Villicum, and can be correlated throughout the study area.

METHODOLOGY

Geologic and geomorphic mapping and detailed topographic surveying of terrace surfaces was conducted along the flanks of Sierra de Villicum. Elevation and form of modern channels were used to constrain the magnitude and style of terrace deformation. Terraces were physically correlated with a suite of dated surfaces to the southwest of the study area (Siame *et al.* 2002). Deformation rates were calculated by assigning ages to the terraces of this study on the basis of the correlation with the dated surfaces to the southwest (Siame *et al.* 2002). A structural model at the crustal scale was developed from field relationships

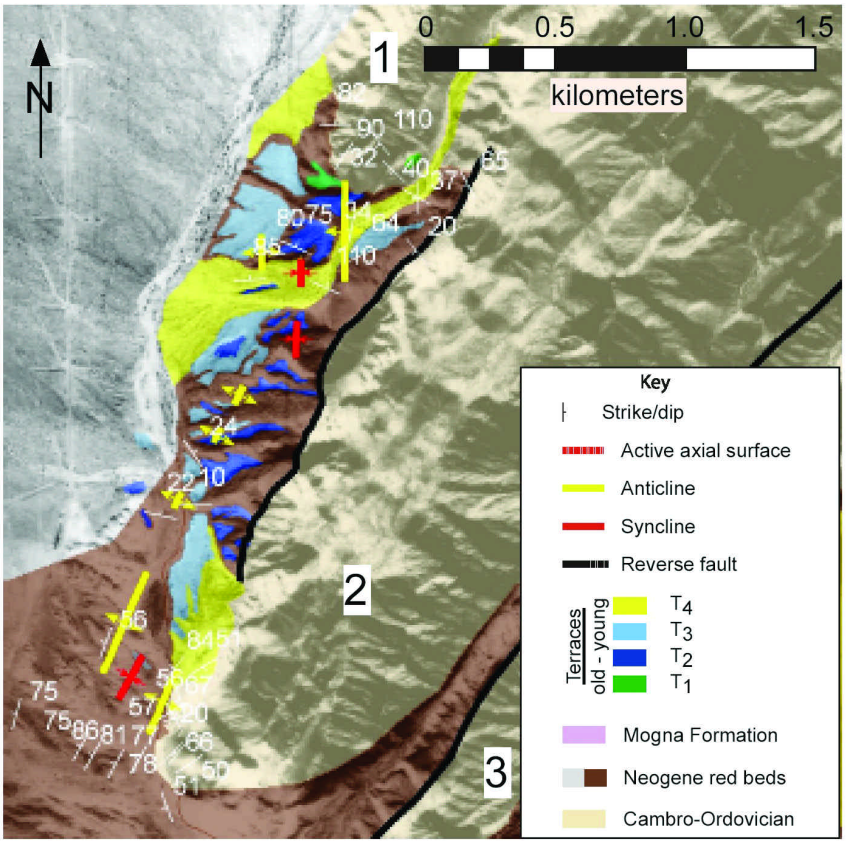

Figure 3: Detailed bedrock and geomorphic map of southwestern end of Sierra de Villicum along the northwestern range front. 1, 2, and 3 mark the three thrust imbricates that duplicate the sequence of Cambro-Ordovician carbonates unconformably overlain by Neogene red beds on southeast-dipping reverse faults. Photos in 4a and b are from imbricate 1 and figures 4c and d are from along the Villicum thrust (VT) along the northwestern margin of imbricate 2. Neither the Villicum thrust nor the thrust on the northwest margin of imbricate 3 continues southwest in the red beds

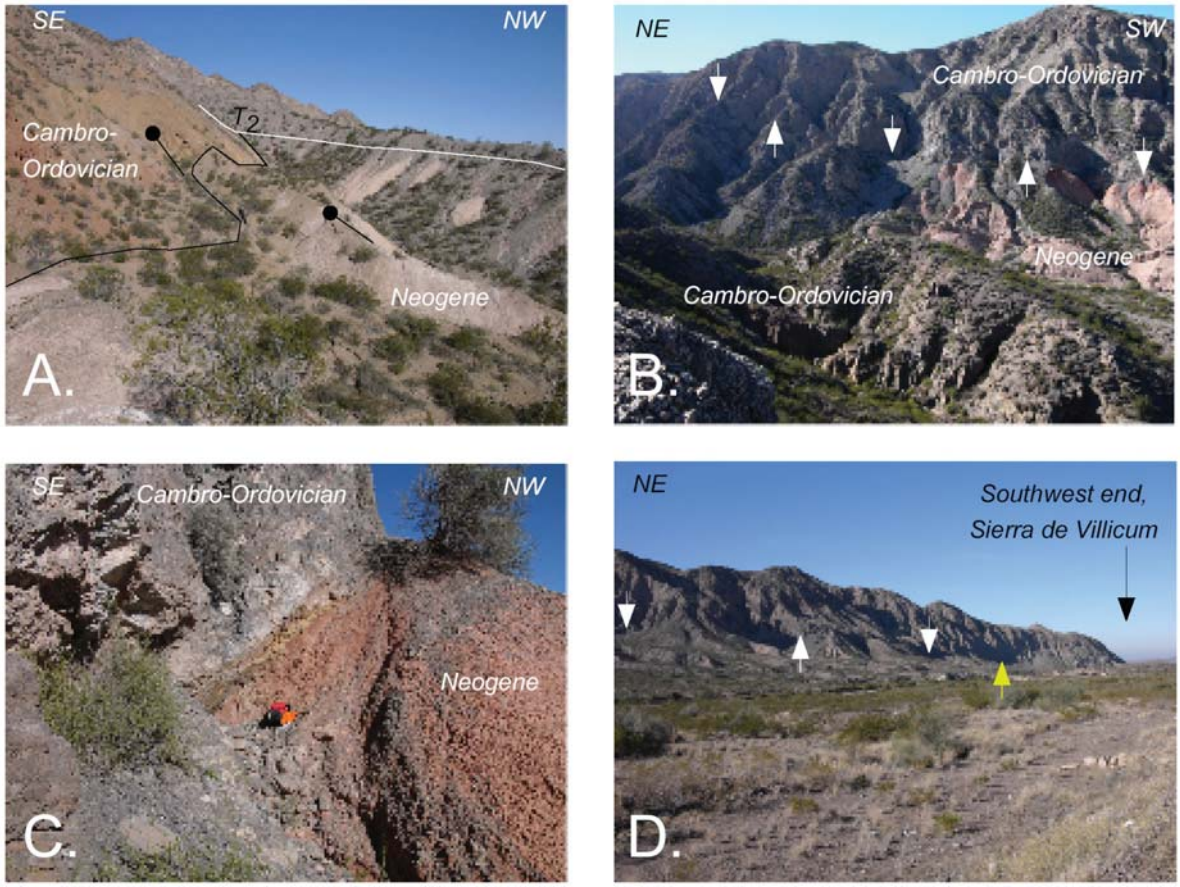

Figure 4: Views of the range-front fault system on the northwest flank of Sierra de Villicum. a) Western-most outcrop is the northwest limb of a fold marked by an unconformable northwest-dipping depositional contact between Cambro-Ordovician strata and Neogene red beds (ball-arrow symbols give dip direction). Terrace gravels of T2 depositionally overlie the contact and are not deformed. b) Cambro-Ordovician and Neogene strata dip southeast in the southeastern limb of the fold. Red beds are truncated by the Villicum reverse fault on the southeast (trace marked by white arrows). c) Dip of Villicum fault varies between 45° and ~50° southeast and has right-oblique shear sense striations on the fault plane. Cambro-Ordovician rocks in the hanging wall are juxtaposed with Neogene rocks in footwall. d) Reverse fault continues at surface to yellow arrow on the southeast (Fig. 3). Southwestward from yellow arrow to the southwestern end of Sierra de Villicum the range-front structure is a fold characterized by northwest-dipping Cambrian unconformably overlain by Neogene red beds. Whereas the fault is well exposed in deeply incised washes along strike, neither scarps nor steps occur in terraces where they overlie the fault trace.

and published microseismicity (Smalley *et al.* 1993). Together, the crustal model and patterns of Quaternary and younger deformation were used to propose a model for the seismogenic source of the 1944 earthquake, to characterize the regional structural style, and to relate the rate and style of crustal deformation to GPS and other data (Brooks *et al.* 2000, Kadinsky-Cade *et al.* 1985, Ramos *et al.* 2002, Smalley *et al.* 1993).

BEDROCK AND TERRACE DEFORMATION, NORTHWEST RANGE FRONT, SIERRA DE VILLICUM

A prominent topographic escarpment marks the northwest range front of Sierra de Villicum. Whereas the range front has been considered a simple thrust contact between Cambro- Ordovician carbonates and Neogene red beds in the hanging wall and footwall of the Villicum thrust, respectively (Siame *et al.* 2002, von Gosen 1992), several thrust imbricates involving the Cambro-Ordovician and Neogene red beds are exposed with both faulted and folded contacts at the range front (Fig. 3). Northwest-dipping carbonates are unconformably overlain by less-steeply tilted red beds in the northwestern-most exposures in the study area (imbricate #1, Figs. 3 and 4a). To the southeast, the carbonates and red beds dip southeast (Fig. 4b). An anticline with a steeply dipping northwest limb and a moderately dipping southeast limb are defined by the contact trace and bed dips (#1, Fig. 3). Red beds in the southeast limb of the anticline are cut by the Villicum thrust, an oblique slip reverse fault (imbricate #2, Figs. 3, 4b, and 4c). The Villicum thrust can be traced in outcrop along strike to the southwest, but disappears into the subsurface and the range front is characterized at the surface by northwest dipping Cambro-Ordovician rocks unconformably overlain by northwest-dipping red beds (Figs. 3 and 4d). This contact traces around the northwest end of Sierra de Villicum, which defines a southwest plunging anticline, the axial trace of which continues to the southwest. Terraces T1-3 are well preserved along the northwest range front (Fig. 3). Both T1 and T2 are continuous across the axial trace of

the northwestern folded unconformity between the Cambro-Ordovician and the Neogene (Figs. 3 and 4a). The terraces extend across the fold axial trace. To the southeast, the Villicum thrust occurs midslope above the elevation of the terraces along the range front (Fig. 4d). Because the Villicum thrust looses elevation to the southwest, however, terrace relationships with faults and bedrock contacts can be resolved (Fig. 3). On the southwest, terraces T2 and T4 continue without scarps across the Villicum fault trace and the northwest-tilted unconformity between the Cambro-Ordovician and Neogene strata. Whereas the Villicum thrust has been interpreted to cut surficial deposits (Siame *et al.* 2002), these field observations indicate that although the range front is characterized by both folded and faulted Cambro-Ordovician and Neogene red beds, neither the folds nor the Villicum fault affect the terraces along the northwestern range front. These observations suggest that the Villicum thrust and range front folds are either inactive or growing imperceptibly on the timescale of development of the terraces. Moreover they reaffirm Whitney's (1991) conclusion, on the basis of detailed mapping on aerial photographs and field mapping, that the fault system along the northwestern range front does not cut terraces of any age.

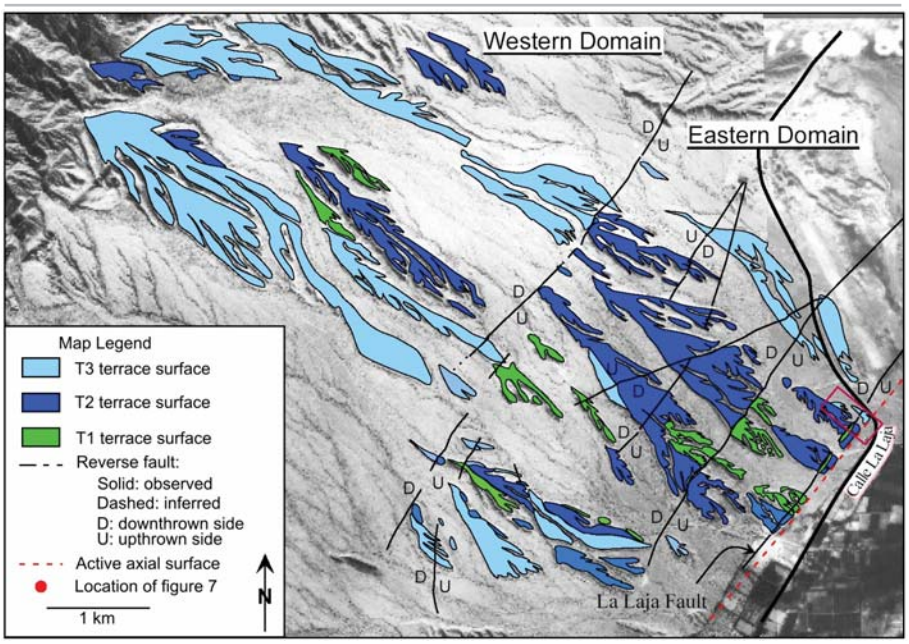

Figure 5: Map of terrace surfaces T1-T3 on the eastern flank of Sierra de Villicum, San Juan, Argentina. Faults and folds that deform terraces define an eastern domain, which contrasts with the western domain where terraces are undeformed. The La Laja fault, which ruptured in the 1944 earthquake (Fig. 7a), and a regionally extensive active axial surface (red dashed line) mark the southeastern edge of the eastern domain. Figures 7b, 7c and 8 depict structural relationships in the wash indicated by the red box near 'Calle La Laja'.

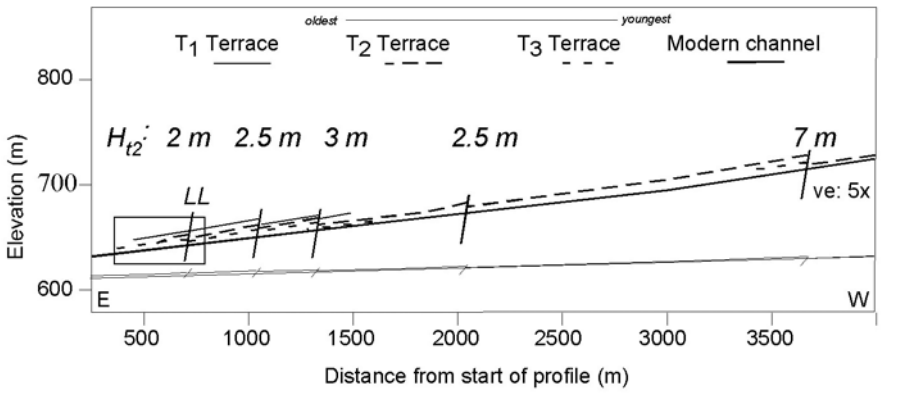

Figure 6: Profile of terraces and modern wash across eastern domain. Faults are steep due to 5x vertical exaggeration (VE) (upper profile; lower profile has no VE). Equivalent horizontal shortening across faults for the T2 surface (Ht2) is calculated from vertical separation and a 40° fault angle. Box indicates structural location of photos in figure 7 and structural data summary of figure 8. LL marks the La Laja fault.

BEDROCK AND TERRACE DEFORMATION, SOUTHEAST FLANK, SIERRA DE VILLICUM

A 10 km-wide panel of shallowly- to moderately-inclined southeast-dipping red beds characterizes the southeast flank of Sierra de Villicum (Fig. 2a). A ~20° angular unconformity marks the contact between the Cambro-Ordovician sediments and the Neogene red beds. Two structural domains can be differentiated within the red beds exposed on the southeastern flank (Fig. 5). Shallow southeast bed dip (<15°) and no faults or small-scale folds characterize the western domain. A laterally continuous southeast dipping thrust fault marks the boundary between the western and eastern domains. Small displacement thrust faults and a southeast-facing monocline are developed throughout the eastern domain (Figs. 2 and 5). Bedding dip changes from 10°-15° to 35°-45° from northwest to southeast, respectively, across the eastern domain. Mogna Formation, the youngest stratigraphically differentiable bedrock unit, is well exposed in three outcrop belts. On the northeast edge of the area the Mogna Formation dips moderately southeast. On the southwest end of the area, in contrast, the Mogna formation dips < 15° and faces south (Fig. 2a). Bedding orientation in the underlying Neogene red beds also changes from southeast facing in the northeast to south facing along strike to the southwest (Fig. 2a).

A low relief topographic surface comprised of a series of fluvial terraces etched into Neogene red beds typifies the southeast flank of the range (Fig. 5). Individual terraces consist of a low-relief bedrock erosio-

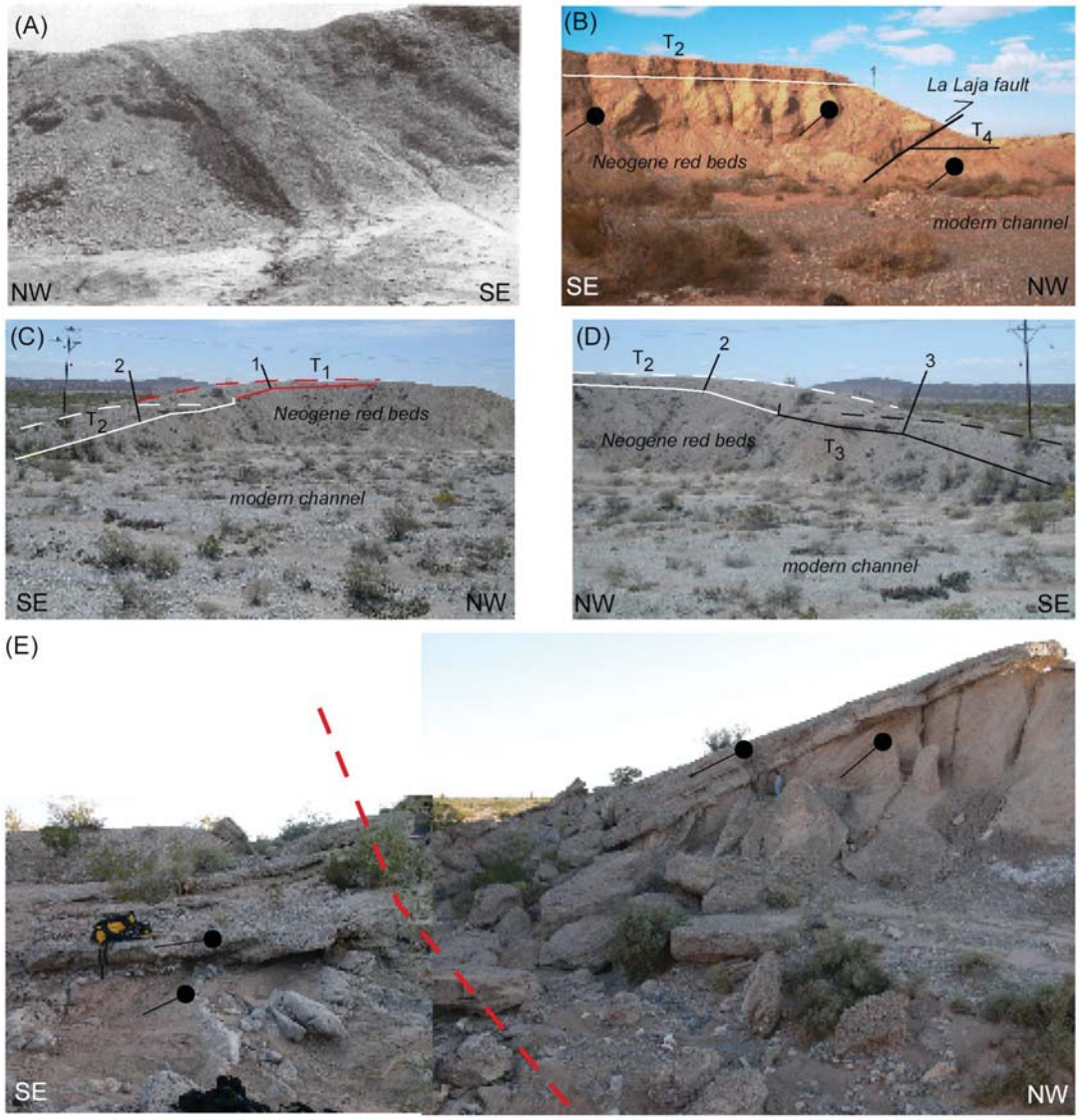

Figure 7: Photos of deformation style on southeastern limit of the eastern domain, southeast flank Sierra de Villicum. (A) Surface rupture on the La Laja fault in 1944 (from Harrington 1944). Resistant beds are inclined at a similar angle to the surface rupture trace. (B) Exposure of La Laja fault southwest of La Laja road. Bed and fault dip (ball-ended arrow) are similar. Terraces 2 and 4 occur in the hanging wall and footwall, respectively. (C) (D) Views to the southwest and northeast of deformed terraces in a wash ~100 m southwest of La Laja road (red dot, Fig. 5). Solid lines mark strath surfaces at the base of terraces; dashed lines mark the abandoned surface. Monoclinal fold hinges within individual terraces do not fold older or younger terraces or underlying Neogene bedrock. Fold hinges in structurally lower and geomorphically lower terraces are located systematically to the southeast of hinges in older, higher surfaces. (E) Synclinal hinge controlling the southeastern break in slope exposed in Neogene bedrock (red dashed line, Fig. 5).

nal surface (a strath), which is overlain by 1-3 meters of poorly sorted limestone-and-dolomite-clast gravels. Map relationships and terrace profiles indicate that the terraces are undeformed in the western domain. Both terrace surfaces and modern channel profiles are concave up and have a nearly constant gradient of ~ 3° across the western domain. In contrast, folds and faults of the eastern domain affect terraces of nearly all ages (Fig. 6). Displacement of terraces across faults varies as a function of age and does not exceed ~10 m for T1. Roughly 17 m of horizontal shortening is deduced from the fault dip and separation of T2 straths across faults in the eastern Domain (Fig. 6).

The most pronounced deformation of terraces is localized in a narrow region near the La Laja fault scarp on the southeastern edge of the eastern domain (Figs. 2, 5 and 7). In this region, the shallowly dipping Neogene strata are tilted to the southeast ~ 40° (Fig. 7). Photographs taken after the 1944 event show that surface rupture on the La Laja fault is approximately parallel to bedding (Fig. 7a) (Harrington 1944). Roughly 60 cm of uplift was measured from a road warped by surface rupture on the fault. Total displacement of individual terrace surfaces is larger than that observed from the 1944 earthquake (Fig. 7b), suggesting that the terrace surfaces provide a com-

posite record of earthquakes prior to and including the 1944 earthquake. Dip of the red bed sequence and the La Laja fault are the same suggesting the fault result from bed-parallel slip during the earthquake (Fig. 7b) (Krugh 2003). Therefore, the La Laja fault is interpreted to be a flexural slip fault (Krugh 2003), which are secondary faults related to folding (Yeats 1986). Folded terraces in the hanging wall to the southeast of the La Laja fault also record deformation related to folding (Figs. 7c-e).

Geometric relationships between individual terraces and underlying bedrock are well exposed in southeast-draining, transverse stream channels (Figs. 5 and 7). Southeast-facing monoclines typified by a change in dip from ~ 3°SE to ~15°-20°SE are present in T1-3 (Figs. 7c and d). Hinges preserved in individual terraces are unique to a given terrace and affect neither younger nor older surfaces. Hinge location change in space systematically as a function of age; the hinge in T3 is located to southeast of T2 (Fig. 7d), which is to the southeast of the T1 hinge (Fig. 7c). Underlying Neogene bedrock is not folded about any of the hinges, in contrast, and has a uniform dip of ~40°SE beneath each of the terraces. A prominent break in slope marks the southeastern limit of the tilted terraces. Terrace T5 is undeformed and inset into older terraces in transverse channels but onlap older surfaces on interfluves. Thus the break in slope is a depositional contact between older, tilted terraces to the northwest and the youngest undeformed terraces on the southeast. Along strike to the northeast, however, a folded unconformity within the Neogene red beds reveals the nature of the same break in slope in terms of bedrock structure. Dip of strata above the unconformity shallows from ~30° to ~10° and from ~60° to ~40° below the unconformity from northwest to southeast, respectively (Fig. 7e). The break in slope is therefore interpreted as the trace of a fold hinge separating more steeply from shallowly southeast dipping strata in the Neogene bedrock. At the structural and stratigraphic level of the terraces, the hinge separates tilted terraces on the northwest from equivalent undeformed sediments on the southeast. The youngest terrace deposits are a thin veneer deposited across the hinge.

TERRACE FOLD MODEL

The observed geometric relationships between bedrock structure, folded terraces, and topography constrain the style of fold growth and shortening rate across the southeastern flank of Sierra de Villicum. Any model for fold growth must account for the principal structural and geomorphic observations along the southeastern edge of the eastern domain, as summarized in figure 8. At the structurally lowest level in the bedrock, bedding changes from shallow to steeper dip across a synclinal hinge that coincides with the topographic break in slope at the southeastern edge of the eastern domain (Figs. 5 and 7e). Bedding to the northwest of the hinge has invariant dip, despite the complex folding of terraces at shallower structural levels. The La Laja fault is a flexural slip fault parallel to bedding (Figs. 7a and b). Terrace folds have a monoclinal geometry marked by a hinge unique to each terrace (Figs. 7c and d). Hinges developed in a terrace of a given age do not affect bedrock or older or younger terraces. Hinge position in space increases with distance northwest from the synclinal hinge as a function of age. A model of fold growth via kink-band migration best reconciles these features (Fig. 9).

Kink-band migration is a mechanism of folding whereby beds change dip due to rotation about axial surface(s) (Suppe 1983, Suppe *et al.* 1997). The region between two corresponding axial surfaces is termed a "kink-band". Fold growth results from migration of one or both axial surfaces defining a kink band, which translates material into the fold limb. In growing structures, one or both of these axial surfaces may move relative to bedrock (Suppe *et al.* 1992). An active axial surface refers to a hinge that moves with respect to rock whereas a fixed axial surface is one that is stationary with respect to rock. As an active axial surface migrates, rock is instantaneously rotated about the axis and translated onto the fold limb. Fold growth rate can be determined when the position of the fixed and active axial surface can be determined in time (Mueller and Suppe 1997, Shaw and Suppe

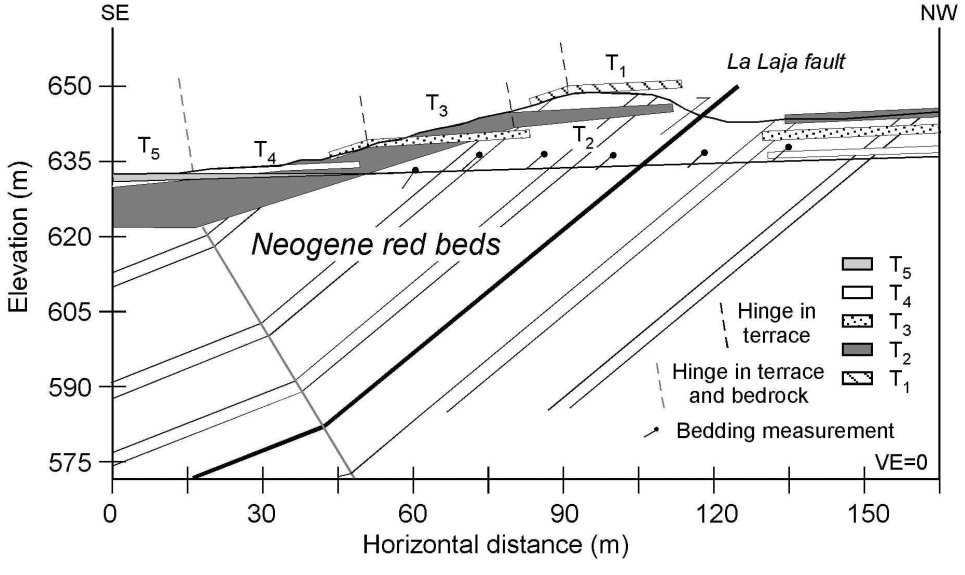

Figure 8: Summary sketch (to scale) of structural relationships in region of wash southwest of La Laja road (red box, Fig. 5; photos in Figs. 7b and c). Topographic profile, T1, T2, and bedding are from ridge on southwest side of wash. T4-5 are from outlet of wash on southeast. T3 projected on to profile from ridge on northeast side wash (Fig. 7c). T2-4 in footwall of the La Laja fault are projected from wash adjacent to the La Laja road (Fig. 5). Bed form lines in Neogene bedrock schematically illustrate bedding. Relationships above ~610 m elevation are observed in the field. Structure below 610 m is pro-jected on the basis of surface data.

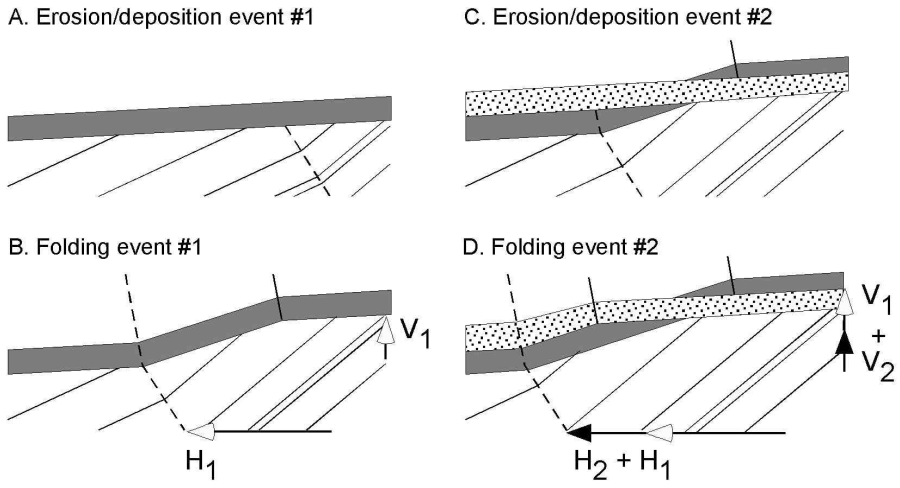

Figure 9: Terrace fold growth model. (A) Fluvial incision cuts a strath terrace into folded bedrock. A thin (1-3 m-thick) gravel layer overlies the strath (grey bar). (B) A fold event deforms the terrace due to a migration of a hinge (dash) through the rock. Strata to the right of the hinge in (A) uplift but do not tilt, whereas strata to the left uplift and tilt, which forms a hinge (solid) fixed within the terrace. Incremental shortening (H1) and uplift (V1) are given by the offset of the hinges and uplift of the strath, respectively (C) Erosion into the fold results in formation of a second terrace, represented by the strath and gravel cap (dotted bar). (D) A second fold event forms a hinge restricted to the second terrace. Total shortening and uplift are equal to the sum of the incremental horizontal (Hn) and vertical (Vn) motion. Compare (D) with figures 6b, 6c, and 7.

1996, Suppe *et al.* 1992).

Strata deposited coevally during fold growth are referred to as syntectonic or growth strata (Riba 1976). Growth strata geometry depends on geometrical changes of fold limbs during folding (DeCelles *et al.* 1991, Ford *et al.* 1997, Suppe *et al.* 1997, Vergés *et al.* 1996). Hinge migration relative to rock and to other hinges dictates growth strata geometry for folds formed due to kink band migration (Suppe *et al.* 1992). For the case of motion of an active axial surface relative to a fixed axial surface, deposition across the fixed hinge results in formation of a new hinge, a growth axial surface, which is fixed with respect to the accumulating growth strata (Suppe *et al.* 1992). At the moment after a bed is deposited, but prior to its incorporation into the fold, the growth and active axial surfaces intersect at a point at the surface. Continued migration of the active axial surface relative to the growth axial surface creates a growth triangle, the size of which is proportional to the total amount of syndepositional fold growth (Suppe *et al.* 1997). Growth axial surfaces, active axial surfaces, and growth triangles thus preserve a record of fold growth because the displacement of the active axial surface relative to the growth axis is represented by their offset in space. Because older growth strata have endured more folding, growth triangle width progressively decreases in younger growth strata.

When sedimentation is unsteady relative to fold growth, such as during punctuated events like earthquake induced folding or climatically variable deposition or erosion, discrete growth axial surfaces form in sediments deposited between growth events (Mueller and Suppe 1997). To illustrate a sequence of alternating erosion/deposition and uplift events and the consequent affect on terraces and bedrock, a simple model of migration of a single active hinge was constructed (Fig. 9). A channel forms a strath as it bevels an erosional surface into titled bedrock and deposits a gravel cap in step 1 (Fig. 9a). Migration of the active hinge by some arbitrary horizontal amount (H1) rotates rock and the terrace as they are drawn into the fold limb, although the amount of rotation is a function of initial dip (Fig. 9b). Incremental folding results in formation of a growth hinge offset a distance H1 with respect to the active hinge. Uplift of the strath at the base of the terrace (V1) depends on H1 and tilt of the bedrock outside of the kink band. Renewed down cutting of the channel forms a new strath/ gravel cap pair comprising a younger terrace (Fig. 9c). A second folding event de-forms the newly formed terrace, creates a growth hinge in the new surface, and the incremental fold growth is given by horizontal offset of the growth hinge with respect to the active hinge and the uplift of the strath relative to the modern channel, H2 and V2, respectively (Fig. 9d). Whereas the cumulative growth is given by the sum of the vertical and horizontal motions, all structures on the side of the hinge opposite to the direction of active hinge migration experience uplift, but no additional tilting. Thus, tilted bedrock and terraces and earlier-formed growth axes are not tilted further during subsequent folding events. The position of a growth axial surface is therefore dependent on the migration rate of the active axial surface relative the time required to form the strath/gravel cap pair of a terrace. Discrete earthquake events are recorded by growth strata formed by kink band migration only under special conditions that include depositional events with greater frequency than folding events, fold growth in scale that exceeds the scale of interseismic sediment accumulation, and structural tilting that is greater than primary depositional dip (of bedding and bed forms).

ACTIVE DEFORMATION AND SHORTENING RATES CROSS THE EASTERN PRECORDILLERA

Active deformation is localized on the southeast flank of Sierra de Villicum (Figs. 2, 3, and 5). No evidence of folding or thrust faulting of terraces is observed along the Villicum thrust fault or folds cropping out along the northwestern range front (Figs. 3 and 4d). In contrast, abundant evidence for active folding is represented on the southeast edge of the southeast flank of Sierra de Villicum (Figs. 5, 6, and 7). The La Laja fault, for example, is a flexural slip fault that ruptured in the 1944 earthquake (Harrington, 1944) and offsets all of the terraces, older terraces have greater vertical separation than younger surfaces (Fig. 8). This later observation argues for the long-term flexural slip faulting accompanying

fold growth in earthquakes. Terraces of all ages are folded as well. A kink-band migration model in which uplift, erosion, and deposition are out of phase fits the geometry of deformed terraces on the southeast flank well (compare Figs. 6, 7 and 8).

Determination of shortening rates across the zone of active folding thus requires absolute age assignments for the various surfaces. To date, no age constraints, unfortunately, are available from the terraces in the study region.

Six kilometers southwest of Sierra de Villicum, however, a suite of three terraces has been dated using cosmogenic radionuclides (Siame *et al.* 2002). Siame *et al.* (2002) mapped terrace surfaces A3, A2, and A1 that are elevated 11±1 m, 6±2 m, and ~0.6 m above the modern channel, respectively. Radionuclide concentrations from A3, A2, and A1 indicate ages of 18.7 - 18.0 ka, 6.9 - 5.3 ka and 1.9 - 1.1 ka, respectively. The terraces are cut into Neogene red beds that are structurally contiguous with the southeastern flank (Fig. 1). Because the terraces of this study and those of Siame *et al.* (2002) occur within the same structural domain, a physical correlation between the two areas was performed to provide estimates on the ages of the terraces in this study. Terraces T1-4 were physical correlated by following terraces up and down channels and across adjacent drainages from the northeast corner of the study area on the southeast flank across strike to the southwestern end of Sierra de Villicum and around to the northwest range front (Fig. 2b). Strath and gravel cap elevation with respect to modern channels form the basis of the correlation.

Uncertainty in the correlation was introduced by correlation across regions with limited preservation of T1-3, correlation across small-displacement faults, by variable elevation of modern channels, and by paleotopography, paleocanyons in particular, preserved between strath surfaces and capping gravels. Uncertainty in the age determinations are introduced because inheritance was not specifically considered in the sampling or subsequent evaluation of the nuclide concentrations (Siame *et al.* 2002). Moreover, inspection of the Siame sampling sites suggests the possibility that one or more of the surfaces are cut-in-fill terraces and therefore have a more complex exposure history than a simple abandoned fill terrace. Either of these two sources of uncertainty implies that the terrace ages may be minimum ages, which means that structural rates based on correlations are maximum values.

Horizontal shortening rates are inverted from the horizontal separation of growth axial surfaces in T1, T2, and T3 relative to the active axial surface to the southwest (Figs. 8-10). On the basis of our terrace mapping, older and younger correlations with the terraces dated with cosmogenic radionuclides of Siame *et al.* (2002) are permissible (Fig. 10). A 'younger' correlation makes T1 equivalent with A3, T2 correlative with A2, and yields a maximum shortening rate of 5 mmyr^{-1} or greater (Fig. 10). An 'older' correlation ties T2 to A3, T3 or T4 to A2, and implies a minimum shortening rate of ~3 mmyr^{-1} (Fig. 10). These rate approximations assume constant shortening since the formation of T2 or T1 for the older and younger correlations, respectively. Independent age determinations in progress for the terraces of this study will provide independent constraint on terrace age and therefore structural rates.

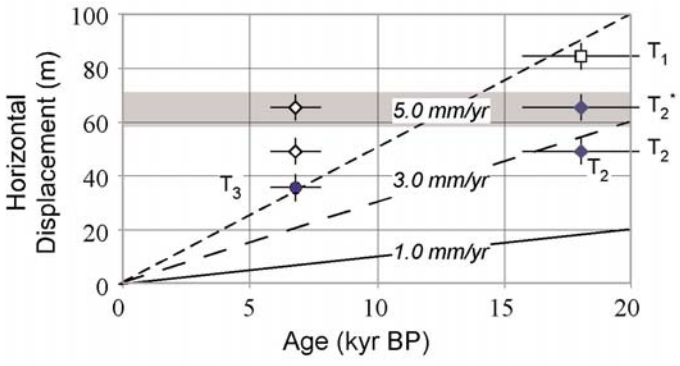

Figure 10: Horizontal shortening rate estimates based on alternative terrace correlations with Siame *et al.* (2002) and horizontal displacement measurements of growth hinge relative to active hinge in terraces and bedrock (Fig. 8). Constant maximum (long dash) and minimum (solid) rates (in millimeters per year (mm/yr)) depend on whether T1 ('younger' correlation, open diamonds) or T2 ('older' correlation, closed diamonds) correlate with Siame's 18.7 ka terrace. Variable shortening rate in time is implied by the 'younger' correlation (short dash). Age error is from Siame *et al.* (2002) (± 2.3 and ± 1.0 ka for 18.7 and 6.8 ka surfaces, respectively). Hinge position is assigned a ± 5 m error.

CRUSTAL SCALE MODEL FOR REFOLDING OF THIN SHINNED THRUST SHEETS BY BASEMENT DEFORMATION

A number of observations suggest that the Sierra de Villicum thrust sheet is being actively refolded. The thrust sheet extends from the Villicum thrust on the northwest to the Tulum Valley syncline on the southeast (Fig. 1). Dip data and stratigraphic contact relationships reveal the presence of a structural high in the middle of the southeast flank of Sierra de Villicum. Dip in the red beds defines a southeast facing monocline characterized by a change from shallowly southeast- to moderately southeast-dipping within the western domain (Fig. 2). Active folding is localized in the moderately dipping limb of the monocline, which is where the La Laja fault and folded terraces are located (Figs. 5 and 8). One key active structure in this region is the active axial surface that crops out in both the terraces and in the bedrock (Figs. 2 and 7). Strike of the contact between the red beds and the overlying Mogna Formation changes from northeast to west along strike from northeast to southwest. In the region where the contact is west striking, both the Mogna Formation and the red beds dip south (Fig. 2b). Together, these observations indicate that the middle of the Sierra de Villicum thrust sheet is marked by a structural high, the structural high is a southeast-facing monocline, and active folding is concentrated on the southeast limb of the monocline (Fig. 11).

A structural high between the Precordillera on the west and the eastern Precordillera on the east is required by structural and stratigraphic relationships (Cristallini and Ramos

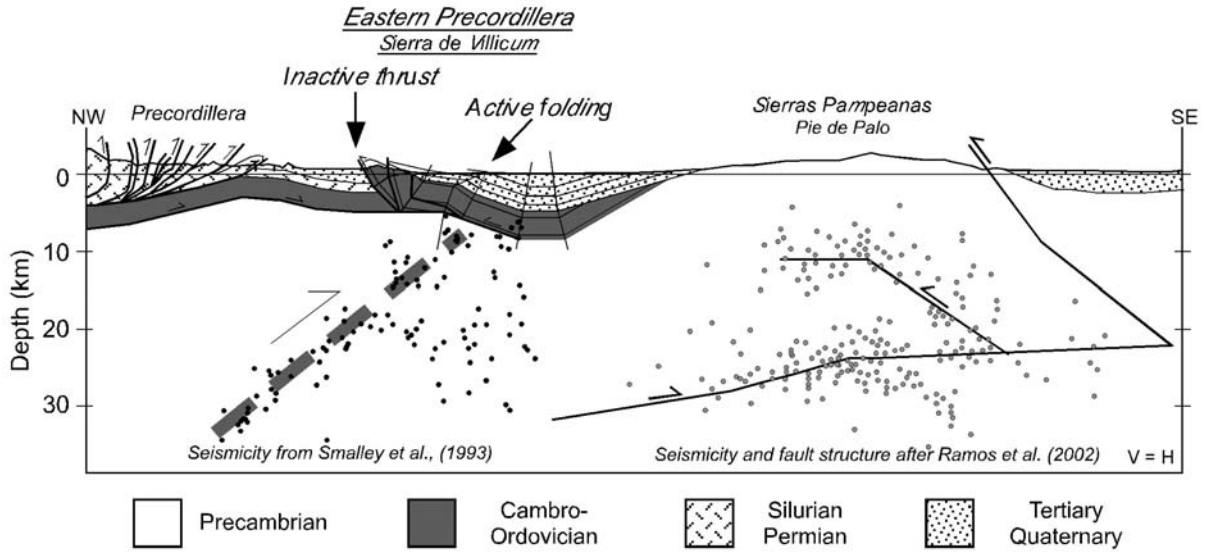

Figure 11: Crustal scale model relating basement seismicity and upper crustal structure beneath the eastern Precordillera. Whereas a thrust sheet carrying Cambro-Ordovician sedimentary cover strata underlies Sierra de Villicum, active deformation is restricted to folding on the southeast flank. Microseismicity between ~5 and 35 km depth defines a northwest-dipping fault plane (black dots) (Smalley *et al.* 1993), which is inferred to be the source of the 1944 San Juan earthquake. Active folding of terraces and flexural slip faulting on the La Laja fault are secondary effects of thrust sheet refolding. A basement high between the Precordillera and the eastern Precordillera is required by the opposing regional dips between the two structural domains. Precordillera structure and stratigraphy are modified from von Gosen (1992). Eastern Precordillera structure is modified from Krugh (2003). Sierras Pampeanas structure and seismicity (light dots) modified from Ramos *et al.* (2002).

2000, Ramos *et al.* 2002, von Gosen 1992). The basal décollement of the Precordillera dips west (Fig. 11). If the hanging wall of the Villicum thrust fault is a hanging wall flat, which is consistent with the dip of the fault and hanging wall bedding (Figs. 3 and 4), the Tulum Valley syncline would represent the down dip branch line of the Villicum thrust system with a regional décollement near the base of the Cambrian Strata (von Gosen 1992). This geometry indicates that the Ullum Valley to the northwest of Sierra de Villicum sits above an arch in the basement separating opposing regional dips of the décollement beneath the Precordillera and eastern Precordillera (Figs. 1 and 11). Microseismicity beneath this region is suggestive of an active fault(s) between 5 and 35 km depth in the basement (Smalley *et al.* 1993). The principal plane revealed by these data is N45E° striking and dips 35° to the northwest (Fig. 11). Focal mechanisms and focal depths of current seismicity indicate active reverse faulting concentrated between 20 and 30 km at depth (Fig. 1b) (Kadinsky-Cade *et al.* 1985, Ramos et al. 2002, Siame *et al.* 2002, Smalley *et al.* 1993). Thus, field relationships, the loci or active deformation, historical seismicity, and microseismicity can be linked in a structural model that relates active refolding of the Sierra de Villicum thrust sheet to an active northwest-dipping fault that extends to the middle crust at depth (Fig. 11).

Four alternative models relate basement faulting in the middle crust with accommodation of slip on upper crustal structures (Fig. 12). A simple fault-propagation fold where the east-facing monocline and structural high between the Precordillera and eastern Precordillera are the forelimb and crest of the fold, respectively, growing above fault tip below the cover sequence (Fig. 12a). Slip from the basement may be transferred to the detachment at the base of the Sierra de Villicum thrust sheet and daylight on the east side of the Tulum Valley syncline (Fig. 12b). Third and fourth alternatives are represented by a wedge geometry whereby east-directed slip on the basement fault is accommodated in the cover sequence by west-directed thrusting (Figs. 12c, d). Transfer of slip to the La Laja fault was first proposed by Smalley *et al.* (1993) to account for the fact that La Laja and basement faults have opposing dips (Fig. 12c). Slip transfer to the Villicum thrust system could also absorb slip at depth on the basement fault (Fig. 12d).

Neither the transfer of slip to a thrust on the east side of the Tulum Valley syncline nor to the La Laja fault is supported by field observation (Figs. 12b, c). No active east vergent faults are present between the west flank of Pie de Palo and the hinge of the Tulum Valley syncline (Fig. 1a) (Ragona *et al.* 1995). Stratigraphic separation across the La Laja fault would have to be proportionate to slip on the basement thrust fault, in the case of the latter alternative, yet field relations suggest that separation is effectively zero (Figs. 7 and 8). Whereas none of the imbricates of the Villicum thrust system apparently affects the terrace sequence, it is possible that shortening on the fault system is reflected at a longer wavelength. Therefore, it is reasonable to conclude that slip on the basement fault system is accommodated by a combination of monoclinal folding above the fault tip, which is potentially accompanied by displacement transfer to one of the faults within the Villicum thrust system (Figs. 12a, d).

We propose that the 1944 earthquake occurred on the northwest-dipping basement fault that extends into the mid-crust beneath Sierra de Villicum. This model contrasts, however, with current models for the 1944 source. Those models propose that the earthquake occurred to the east of Sie-

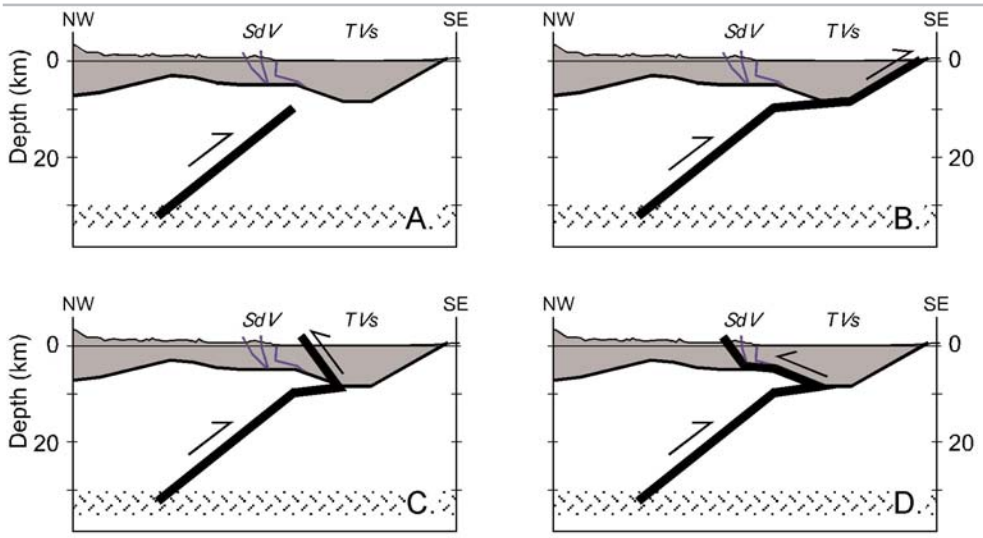

Figure 12: Alternative models for the accommodation of slip in the cover sedimentary rocks (grey shading) due to fault displacement on the basement reverse fault. A) Fault slip is accommodated by fault-propagation folding above the fault tip. (B) Fault slip is transfered to a fault system beneath the Tullum Valley syncline (TVs). (C) Fault slip is transfered to the La Laja fault on the east flank of Sierra de Villicum (SdV). (D) Fault slip is transferred to the imbricate fan thrust system bounding the west flank of Sierra de Villicum. Depth of seismicity is indicated by cross-hatched pattern (after Smalley and Isacks 1990).

rra de Villicum on an east-dipping fault system that extends into the basement (Alvarado and Beck 2006, Perucca and Paredes 2000, 2002, Siame *et al.* 2002). An earthquake source on an east dipping fault system is based on the inference that the Villicum thrust system ruptured in the 1944 event and is therefore the up-dip continuation of a fault that extends to ~20 km depth beneath the Tulum Valley (Siame *et al.* 2002). Others contend that because of the surface rupture in the earthquake, the east-dipping La Laja fault is the up-dip continuation of the seismogenic fault (Alvarado and Beck 2006, Perucca and Paredes 2000, 2002, Smalley *et al.* 1993). A source on an east-dipping fault is consistent with two of the three reported locations for the epicenter of the 1944 earthquake, which lie to the southeast of Sierra de Villicum (Fig. 1) (Alvarado and Beck 2006). The La Laja fault can be connected with a hypocenter at ~11 km depth beneath the Tulum Valley, which was determined via an inversion of historic seismograms based on assuming apriori that epicenter is to the east (Alvarado and Beck 2006). In this model the La Laja fault is an imbricate splay off the fault system proposed in the Siame *et al.* (2002) model.

A number of observations can be used to evaluate the competing structural models for the eastern Precordillera and therefore the potential seismic sources for the 1944 event. The key observations include the relative activity and style of faulting on the Villicum and La Laja faults, the location and geometry of active folding and faulting, alternative epicentral locations for the 1944 earthquake, and the regional distribution of seismicity with depth. Field data indicate that the Villicum thrust system is either inactive or moving at a rate slower than can be recorded by geomorphic markers, given that none of the individual thrust imbricates of the fault systems cuts or folds terraces of any age (Figs. 3 and 4). Although there is no field evidence for active slip along the fault trace, it is possible that some slip on the thrust may accumulate as the consequence of folding or slip transfer from the basement fault (Fig. 12). Bedding-fault relationships across the La Laja fault are consistent with a flexural slip interpretation of the active faulting (Figs. 7a, 7b, and 8). Thus, surface rupture of the La Laja fault reflects coseismic fold growth and not surface rupture of the primary seismogenic fault, which is consistent with the location of the fault within the actively growing monocline.

Bedrock and terrace geometries indicate that the east-facing monocline is refolding the Sierra de Villicum thrust sheet (Figs. 2 and 11). A model where the active deformation at the surface is dominated folding above a northwest dipping basement thrust reconciles the fold-related flexural slip faulting on the La Laja fault, bedrock and terrace structural relationships, and the spatial distribution of active structures. A fault that extends westward to ~35 km depth, as suggest by microseismicity (Smalley *et al.* 1993), is consistent with an epicentral location to the west of Sierra de Villicum (Fig. 1), which is one of three proposed locations (Alvarado and Beck 2006). Moreover, the majority of earthquakes occur between 20 and 30 km (Fig. 1b) (Smalley and Isacks 1990). If the hypocenter of the earthquake is shallow (~11 km) and to the east of Sierra de Villicum, as suggested by the epicentral locations in the vicinity of San Juan (Fig. 1) and the inversion of historic seismograms (Alvarado and Beck 2006), the west-dipping crustal fault proposed here represents a second and previously unrecognized active seismic source in the boundary region between the Precordillera and Sierras Pampeanas.

Global positioning system (GPS) data indicate that the rate of convergence of the Precordillera with respect to the Sierras Pampeanas across the eastern Precordillera is ~4.5 $mmyr^{-1}$ (Brooks *et al.* 2003), which provides a framework for evaluating shortening rates determined from the deformed terraces. Horizontal shortening rate across the southeastern flank of Sierra de Villicum is estimated to be no more than 3 $mmyr^{-1}$ (Fig. 10). That rate is determined from the sum of shortening of local folding of terraces where the folding is being forced by a local change in dip (Fig. 8) and by the displacement of faults in the eastern domain (Figs. 5 and 6) (Krugh 2003), of a regionally extensive long-wavelength monocline (Fig. 11). If the fold is growing via kink band migration, the horizontal component of fold growth is controlled by the underlying fault orientation and slip rate (Suppe

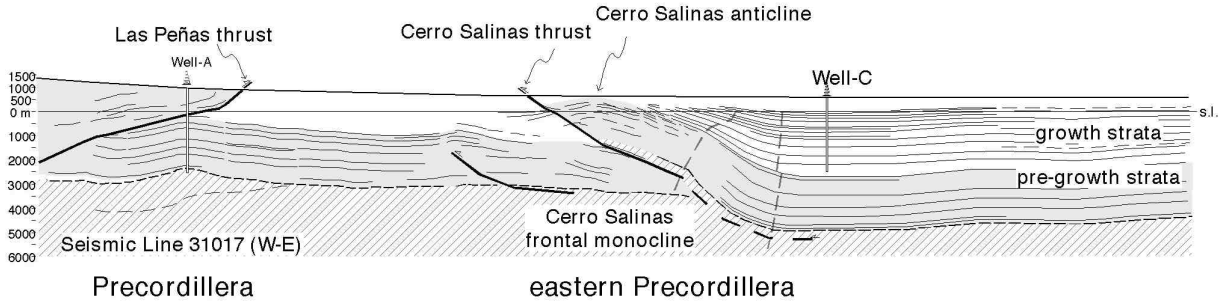

Figure 13: Interpretation of seismic line 31017 from Repsol-YPF (from Vergés *et al.* 2002). The Las Peñas thrust marks the leading edge of the Precordillera thin-skinned thrust belt and is active (Costa *et al.* 2000). Note that Cerro Salinas has an east-facing monoclinal geometry in the center of the thrust sheet. The basement is shallower on the west than it is on the east. Growth strata document the long-term growth of the fold.

et al. 1992).

Shortening at ~3 mmyr^{-1} across the eastern Precordillera due basement thrust faulting is consistent with seismicity and short- and long-term shortening rates measured regionally. Evidence of active folding and faulting is present across Pie de Palo to the east of Sierra de Villicum (Fig. 1a) (Ramos *et al.* 2002). Shortening rate across Pie de Palo is of 4 mmyr^{-1} since 3 Ma (Ramos *et al.* 2002), The sum of the rates across Pie de Palo and Sierra de Villicum (~7 mmyr^{1}) are consistent with, albeit higher, than the GPS-determined rate change between the Precordillera and the Sierras Pampeanas (4.5 mmyr^{-1}, Brooks *et al.* 2003). If the sum of the two rates represents the long term regional shortening rate, despite the fact that rates are measured over different timescales, it seems likely that the ~3 mmyr^{-1} horizontal rate across the eastern Precordillera is a maximum estimate (Figs. 8 and 9). Independent age determinations for the terraces in the study are will provide better constraints on the deformation rates within the eastern Precordillera. Shortening rate at 31° S north of the study area is ~5 mmyr^{-1} since 2.7 Ma (Zapata and Allmendinger 1996a). Seismicity is focused beneath the eastern Precordillera and Sierras Pampeanas region (Alvarado and Beck 2006, Kadinsky-Cade 1985, Kadinsky-Cade *et al.* 1985, Siame *et al.* 2005, Smalley and Isacks 1990, Smalley *et al.* 1993), which supports the inference that active deformation is concentrated deformation in eastern Precordillera-western Sierras Pampeanas region.

Fault dip is a key difference between the crustal model proposed in this study and the structural model used to interpret the GPS velocity field. An elastic model of the GPS data using a 10° west dipping plane fits well the velocity gradient across the Precordillera-Sierras Pampeanas transition (Brooks *et al.* 2003). The rationale for this geometry is a cross-section across the Bermejo basin north of 31° S (Zapata and Allmendinger 1996a). A key feature of this model of the GPS velocity field is that the model fault represents the basal décollement of the Precordillera (Brooks *et al.* 2003). At 32° S in the study area, however, there is little evidence that the frontal thrust of the Precordillera is active. Historical seismicity, recent earthquakes, and the crustal scale model presented here suggest that active structures involve the basement to depths of ~35 km (Figs. 1 and 10) (Costa *et al.* 2000, Costa *et al.* 1999, Kadinsky-Cade *et al.* 1985, Ramos *et al.* 2002, Smalley *et al.* 1993). Active, strain-accumulating faults that continue at moderate dips to depths of ~35 km are permissible from the perspective of the GPS velocity field given that the fact the data are consistent with a range of model fault dips (Brooks *et al.* 2003).

Other thrust sheets in the eastern Precordillera have similarities with the Villicum thrust sheet. Cerro Salinas is an isolated outcrop of Cambro-Ordovician carbonates unconformably overlain by Neogene red beds (Fig. 1) (Comínguez and Ramos 1991, Vergés *et al.* 2002). An east-dipping thrust fault marks the western boundary of the thrust sheet and both long-term and active folding are concentrated on the eastern, down-dip end of the thrust sheet (Fig. 13). A monoclinal geometry marks the style of folding and the geometry of growth strata in the red beds is consistent with fold growth due to kink band migration. The basement, be-low the basal décollement is structurally higher in the footwall on the west than it is beneath the undeformed foreland on the east (Fig. 13). Cerro Salinas is apparently underlain and folded by an antiform that involves the basement. Moreover, active deformation is concentrated in the east, which is the forelimb of the fold, rather than on the west along the surface trace of the thin-skinned thrust sheet. Thus, the model for basement faulting proposed for Sierra de Villicum (Fig. 11) may also apply to Cerro Salinas (Fig. 13), which suggests that the structural style of active deformation in the boundary region between the thin- and thick-skinned Precordillera and Sierras Pampeanas provinces involves active basement-involved thrusting that is overprinting earlier-formed thin-skinned thrust sheets. The onset of this transition is uncertain, but has implications for seismic sources for large cities in western Argentina that lie in the foothills of the Andes.

CONCLUSIONS

1. The principal structure in the eastern Precordillera northwest of San Juan, Argentina is a southeast dipping thrust sheet beneath Sierra de Villicum, which is bound at the base on the northwest by the Villicum reverse fault along the range front and on the southeast by the Tulum Valley syncline. Cambro-Ordovician carbonates unconformably overlain by Neogene red beds comprise the bedrock of the thrust sheet.

2. A suite of 5 fluvial terraces beveled into Neogene red bed bedrock provide markers that allow the late Quaternary deformation in the eastern Precordillera at ~32° to be characterized.

3. The Villicum thrust system along the northwestern range front of Sierra de Villicum juxtaposes thrust imbricates of folded Cambro-Ordovician carbonates against Neogene red beds. All the field evidence indicates that (A) none of the imbricate thrusts extends southwest of the Paleozoic rocks holding up Sierra de Villicum, (B) the terraces overlie faults of the thrust system, and (3) no fault scarps are preserved in terraces of any age.
4. Active deformation in the eastern Precordillera at 32° is localized on the southeastern flank of Sierra de Villicum, in the middle of the Villicum thrust sheet.
5. A number of active small displacement active faults cut fluvial terraces. A narrow, well-defined region on the southeast flank of Sierra de Villicum contains evidence of folding, which includes the La Laja fault that ruptured in the 1944 San Juan earthquake.
6. Evidence for active folding includes flexural slip faulting on the La Laja fault, which is a bedding parallel fault in the Neogene bedrock that cuts terraces of all ages. The oldest three terraces (T1-3) are folded and the fold geometry is characterized by monoclinal form. Individual terraces are folded about hinges that are unique to that terrace and affect neither older nor younger terraces or bedrock. Hinges in younger terraces are located to the southeast with respect to hinges in older terraces.
7. A kink band model of fold growth satisfies all of the key field observations at the structural level of the bedrock and the terraces. From this model the shortening since abandonment of the oldest terrace, T1, can be estimated.
8. Correlation with dated terraces roughly 15 km to the southwest (18.7-18.0 ka. 6.8-5.8 ka, and 1.9-1.1 ka) (Siame *et al.* 2002) allows for older and younger age assignments for terraces T1-3 of this study. Maximum shortening rate across the eastern Precordillera is ~3 $mmyr^{-1}$, as determined from the integration of the fold model and terrace correlation. These rates are consistent with short-term rates determined from GPS (Brooks *et al.* 2003) and with long-term rates determined via cross-sections and growth strata to the north of 31° S (Zapata and Allmendinger 1996a).
9. The loci of active folding, dip data and bedrock contacts suggest that the Sierra de Villicum thrust sheet is being actively folded by a deeper structure. A crustal model is proposed to reconcile the pattern of folding of the thrust sheet, a northwest-dipping zone of microseismicity, and a structural high in the basement between the Precordillera on the west and eastern Precordillera on the east. In this model, active deformation of the eastern Precordillera is a function of folding of upper crustal thin-skinned structures due to slip on a northwest-dipping blind thrust fault that extends to ~35 km depth.
10. Near surface structures record active folding and coseismic faulting during the 1944 earthquake, which implies that the basement reverse fault is the source of the 1944 San Juan earthquake.
11. Basement rocks beneath Cerro Salinas, another eastern Precordillera thrust sheet to the southwest, are also characterized by an antiformal geometry, which suggests that blind thrust faulting on east-vergent basement faults represents a significant, underappreciated seismic hazard in western Argentina.

ACKNOWLEDGMENTS

Drs. Ernesto Cristallini and Matias Ghiglione provided careful and thoughtful reviews that improved the quality of this work. Carlos Costa, Daniel Ragona, Robert Yeats, and Emily Schultz are thanked for numerous discussions of this paper and the seismotectonics of western Argentina. AJM was supported by U.S NSF grants EAR-0232603and EAR-0409443 and a Research Equipment Reserve Fund grant from Oregon State University. We thank Repsol-YPF S.A. for providing us with the seismic line and for the permission to publish it (Fig. 13). J.V. was partially supported by 99AR0010 CSIC-CONICET project and Grups de Recerca Consolidats (II Pla de Recerca de Catalunya) Projects 1997 SGR 00020.

WORKS CITED IN THE TEXT

Alvarado, P. and Beck, S. 2006. Source characterization of the San Juan (Argentina) crustal earthquakes of 15 January 1944 (M7.0) and 11 June 1952 (M6.8). Earth and Planetary Science Letters 243(3-4): 615-631.

Bastias, H. E., Weidmann, N. E. and Perez, A. M. 1985. Dos zonas de fallamiento Pliocuaternario en la Precordillera de San Juan Translated: The Plio-Quaternary fault zone in the Precordillera of San Juan. 9°Congreso Geológico Argentino, Actas 2: 329-341.

Brooks, B. A., Bevis, M., Smalley, R., Kendrick, E., Manceda, R., Lauria, E., and Araujo, M. 2003. Crustal motion in the southern Andes (26°-36° S): Do the Andes behave like a microplate? Geochemistry, Geophysics, Geosystems 4(10): 1-14.

Comínguez, A. H. and Ramos, V. A. 1991. La estructura profunda entre Precordillera y Sierras Pampeanas de la Argentina: Evidencias de la sísmica de reflexión profunda. Revista Geológica de Chile 18: 3-14.

Costa, C. H., Gardini, C. E., Diederix, H., and Cortés, J. M. 2000. The Andean orogenic front at Sierra de Las Peñas-Las Higueras, Mendoza, Argentina. Journal of South American Earth Sciences 13(3): 287-292.

Costa, C. H., Rockwell, T. K., Paredes, J. D., and Gardini, C. E. 1999. Quaternary deformations and seismic hazard at the Andean orogenic front (31°-33°, Argentina): a paleoseismological perspective. 4° International Symposium on Andean Geodynamics (Goettingen), Proceeding 187-191.

Costa, C. H. and Vita-Finzi, C. 1996. Late Holocene faulting in the Southeast Sierras Pampeanas of Argentina. Geology 24(12): 1127-1130.

Cristallini, E. O. and Ramos, V. A. 2000. Thick-skinned and thin-skinned thrusting in the La Ramada fold and thrust belt; crustal evolution of the High Andes of San Juan, Argentina (32° SL). Tectonophysics 317 (3/4): 205-235.

DeCelles, P. G., Gray, M. B., Ridgway, K. D., Cole, R. B., Srivastava, P., Pequera, N., and Pivnik, D. A. 1991. Kinematic history of a foreland uplift from Paleocene synorogenic conglomerate, Beartooth Range, Wyoming and Montana. Geological Society of America Bulletin 103: 1458-1475.

Fielding, E. J. and Jordan, T. E. 1988. Active deformation at the boundary between the Precordillera and Sierras Pampeanas, Argentina, and comparison with ancient Rocky Mountain deformation. Geological Society of America, Memoir 171: 143-163.

Ford, M., Artoni, A., Williams, E. A., Vergés, J., and Hardy, S. 1997. Progressive evolution of a fault propagation fold pair from growth strata geometries, Sant Llorenç de Morunys, SE Pyrenees. Journal of Structural Geology 19(3-4): 413-441.

González Bonorino, F. 1950, Algunos problemas geológicos de las Sierras Pampeanas: Revista de la Asociación Geológica Argentina 5: 81-110.

Groeber, P. 1944. Movimientos tectónicos contemporáneos y un nuevo tipo de dislocaciones: Notas del Museo de La Plata 9(33): 363-375.

Harrington, H. J. 1944. El sismo de San Juan; del 15 de Enero de 1944. Corporación para la promoción del intercambio, S. A., 79 p., Buenos Aires.

Jordan, T. E. and Allmendinger, R. W. 1986, The Sierras Pampeanas of Argentina; a modern analogue of Rocky Mountain foreland deformation. American Journal of Science 286 (10): 737-764.

Jordan, T.E., Isacks, B., Ramos V.A., and Allmendinger, R.W. 1983a. Mountain building in the Central Andes. Episodes 1983(3): 20 26, Ottawa.

Jordan, T. E., Isacks, B. L., Allmendinger, R. W., Brewer, J. A., Ramos, V. A., and Ando, C. J. 1983 b. Andean tectonics related to geometry of subducted Nazca Plate: Geological Society of America Bulletin 94(3): 341-361.

Kadinsky-Cade, K. 1985. Seismotectonics of the Chile margin and the 1977 Caucete earthquake of western Argentina. PhD Dissertation, Cornell University, 253 p.

Kadinsky-Cade, K., Reilinger, R., and Isacks, B. 1985. Surface deformation associated with the November 23, 1977, Caucete, Argentina, earthquake sequence. Journal of Geophysical Research B90(14): 12,691-12,700.

Krugh, W. C. 2003. Fold growth due to kink-band migration in repeated earthquakes, Sierra de Villicum, San Juan, Argentina. Master's thesis, Oregon State University, 54 p.

Mueller, K. and Suppe, J. 1997. Growth of Wheeler Ridge anticline, California: geomorphic evidence for fault-bend folding behavior during earthquakes. Journal of Structural Geology 19(3-4): 383-386.

Paredes, J. D. and Uliarte, E. 1988. Análisis morfotectónico del sistema de fallamiento Precordillera oriental, San Juan, Argentina. 2° Reunión Sudamericana del Proyecto 206 del IGCP, Santiago.

Perucca, L. P. and Paredes, J. D. 2000. Fallamiento activo y su relación con la magnitud máxima del sismo probable en la zona de la laja. Departamento Albardón. San Juan. República Argentina. 9° Congreso Geológico Chileno, Actas 4 p.

Perucca, L. P. and Paredes, J. D. 2002. Peligro sísmico en el departamento Albardón y su relación con el área de fallamiento La Laja, provincia de San Juan. Revista de la Asociación Geológica Argentina 57(1): 45-54.

Ragona, D., Anselmi, G., González, P., and Vujovich, G. 1995. Mapa Geológico de la Provincia San Juan, República Argentina: Ministerio de Economía y Obras y Servicios Públicos, scale 1:500,000.

Ramos, V. A., Cristallini, E. O., and Perez, D. J. 2002. The Pampean flat-slab of the central Andes. Journal of South American Earth Sciences 15(1): 59-78.

Riba, O. 1976. Syntectonic unconformities of the Alto Cardener, Spanish Pyrenees: A genetic interpretation. Sedimentary Geology 15: 213-233.

Shaw, J. H. and Suppe, J. 1996. Earthquake hazards of active blind-thrust faults under the central Los Angeles basin, California. Journal of Geophysical Research 101(B4): 8623-8642.

Siame, L. L., Bellier, O., Sebrier, M., Bourles, D., L., Leturmy, P., Perez, M., and Araujo, M. 2002. Seismic hazard reappraisal from combined structural geology, geomorphology and cosmic ray exposure dating analyses; the eastern Precordillera thrust system (NW Argentina). Geophysical Journal International 150(1): 241-260.

Siame, L. L., Bellier, O., Sebrier, M., Bourles, D., L., Leturmy, P., Perez, M., and Araujo, M. 2005. Corrigendum - Seismic hazard reappraisal from combined structural geology, geomorphology and cosmic ray exposure dating analyses; the eastern Precordillera thrust system (NW Argentina). Geophysical Journal International 161(2): 416-418.

Smalley Jr., R. and Isacks, B. L. 1990. Seismotectonics of thin- and thick-skinned deformation in the Andean foreland from local network data; evidence for a seismogenic lower crust. Journal of Geophysical Research 95 (B8): 12,487-12,498.

Smalley, R., Jr., Pujol, J., Regnier, M., Chiu, J.-M., Chatelain, J.-L., Isacks, B. L., Araujo, M., and Puebla, N. 1993. Basement seismicity beneath the Andean Precordillera thin-skinned thrust belt and implications for crustal and lithospheric behavior. Tectonics 12(1): 63-76.

Suppe, J. 1983. Geometry and kinematics of fault bend folding. American Journal of Science 283: 648-721.

Suppe, J. S., Chou, G. T., and Hook, S. C. 1992, Rates of folding and faulting determined from growth strata. In McClay, K. R. (ed.) Thrust Tectonics, Chapman and Hall, p. 105-122, London.

Suppe, J., Sàbat, F., Muñoz, J. A., Poblet, J., Roca, E., and Vergés, J. 1997. Bed-by-bed fold growth by kink-band migration: Sant Llorenç de Morunys, eastern Pyrenees. Journal of Structural Geology 19(3-4): 443-461.

Vergés, J., Burbank, D. W., and Meigs, A. J. 1996. Unfolding: An inverse approach to fold kinematics. Geology 24: 175-178.

Vergés, J., Ramos, V.A., Bettini, F., Meigs, A., Cristallini, E., Cortés, J. M., and Dunai, T. 2002. Geometría y edad del anticlinal fallado de Cerro Salinas. 15° Congreso Geológico Argentino, Actas 3: 290-295, Calafate.

Von Gosen, W. 1992. Structural evolution of the Argentine Precordillera; the Rio San Juan section. Journal of Structural Geology 14(6): 643-667.

Whitney, R. A. 1991. Faulting and Tectonics in the Foreland Basin Fold/Thrust Belt of the San Juan Province, Argentina, and a Comparison of the Yakima Fold/Thrust Belt of the Northwestern United States. Ph.D. thesis, University of Nevada-Reno, 176 p.

Yeats, R. S. 1986. Active faults related to folding In Wallace, R. E. (ed.) Active Tectonics, National Academy Press: 63-79, Washington.

Zapata, T. R. and Allmendinger, R. W. 1996 a. Growth stratal records of instantaneous and progressive limb rotation in the Precordillera thrust belt and Bermejo basin, Argentina. Tectonics 15: 1065-1083.

Zapata, T. R. and Allmendinger, R. W. 1996 b. Thrust-front zone of the Precordillera, Argentina; a thick-skinned triangle zone. American Association of Petroleum Geologists, Bulletin 80(3): 359-381.

Recibido: 30 de junio, 2006
Aceptado: 15 de noviembre, 2006